A New Conformal FDTD(2,4) Scheme for Modeling Three-Dimensional Curved Perfectly Conducting Objects

Wei Sha, Xianliang Wu, Zhixiang Huang, and Mingsheng Chen

***Abstract*—A new high-order conformal FDTD(2,4) scheme is proposed to solve the electromagnetic scattering from 3-D curved perfectly conducting objects. For electric field components, the update equations do not need to be modified. For magnetic field components, the inner loop is treated with the locally conformal technique, and the outer loop is unmodified. Numerical results demonstrate that the high-order conformal scheme can obtain better numerical precision under coarse grid condition compared with the low-order conformal method and the high-order staircasing approach, which in turn saves CPU time and memory.**

***Index Terms*—Conformal technique, electromagnetic scattering, high-order difference, staircasing approach.**

I. Introduction

THE traditional finite-difference time-domain (FDTD) method [1], which is explicit second-order-accurate in both space and time, has been widely applied to electromagnetic computation and simulation. However, the FDTD method has two primary drawbacks. One is the inability to accurately model curved complex surfaces and material discontinuities by using the staircasing approach with structured grids, and another is the significant accumulated errors from numerical dispersion and anisotropy. Hence fine grids are required to obtain satisfying numerical results, which leads to vast memory requirements and high computational costs, especially for electrically-large domains and for long-term simulation.

For solving the first problem, a variety of conformal techniques have been proposed in [2]–[6]. For solving the second problem, Fang put forward the staggered FDTD (2,4) scheme [7], which can save computational resources by using coarse grids. However, how to model the curved surfaces with the high-order difference is an open question. In other words, is it possible that we can obtain both high accuracy and low dispersion under curved boundary and coarse grid conditions?

In order to achieve the goal, the one-sided difference [8] was studied. However, the strategy did not seem to consider the shape of objects. Another method is the hybrid subgridding technique [9]. Yet it must adopt spatial and temporal interpolation strategies to eliminate the spurious reflections between the coarse grids and the fine grids.

Manuscript received September 15, 2007; revised October 5, 2007. This work was supported in part by the National Natural Science Foundation Of China under Grant 60671051.

The authors are with the Key Laboratory of Intelligent Computing and Signal Processing, Anhui University, Hefei 230039, China (e-mail: ws108@ahu.edu.cn).

Digital Object Identifier 10.1109/LMWC.2008.916772

In this letter, we propose a new high-order conformal FDTD (2,4) scheme to solve the electromagnetic scattering from 3-D curved perfectly conducting objects. The scheme can obtain satisfying numerical results under coarse grid condition without spatial or temporal interpolation.

II. High-Order Conformal Scheme

The electric field components depend on the magnetic field components, hence we only modify the update equations of the magnetic fields, and keep those of electric fields unmodified.

The update equation for the proportional $\hat{E}_x \left(\hat{E}_x = E_x\sqrt{\varepsilon_0/\mu_0}\right)$ field is given as

$$\begin{aligned}\hat{E}_x^{n+1}\left(i+\frac{1}{2},j,k\right) = {} & \hat{E}_x^{n}\left(i+\frac{1}{2},j,k\right)\\ \Bigg\{ & +\alpha_{y1}\times\left[H_z^{n+1/2}\left(i+\frac{1}{2},j+\frac{1}{2},k\right)-H_z^{n+1/2}\left(i+\frac{1}{2},j-\frac{1}{2},k\right)\right]\\ & -\alpha_{z1}\times\left[H_y^{n+1/2}\left(i+\frac{1}{2},j,k+\frac{1}{2}\right)-H_y^{n+1/2}\left(i+\frac{1}{2},j,k-\frac{1}{2}\right)\right]\\ & +\alpha_{y2}\times\left[H_z^{n+1/2}\left(i+\frac{1}{2},j+\frac{3}{2},k\right)-H_z^{n+1/2}\left(i+\frac{1}{2},j-\frac{3}{2},k\right)\right]\\ & -\alpha_{z2}\times\left[H_y^{n+1/2}\left(i+\frac{1}{2},j,k+\frac{3}{2}\right)-H_y^{n+1/2}\left(i+\frac{1}{2},j,k-\frac{3}{2}\right)\right]\Bigg\}\end{aligned} \tag{1}$$

$$\alpha_{y1} = \frac{9}{8}\times CFL_y, \quad \alpha_{z1} = \frac{9}{8}\times CFL_z \tag{2}$$

$$\alpha_{y2} = \frac{-1}{24}\times CFL_y, \quad \alpha_{z2} = \frac{-1}{24}\times CFL_z \tag{3}$$

$$CFL_y = \frac{1}{\sqrt{\mu_0\varepsilon_0}}\frac{\Delta_t}{\Delta_y}, \quad CFL_z = \frac{1}{\sqrt{\mu_0\varepsilon_0}}\frac{\Delta_t}{\Delta_z} \tag{4}$$

where Δ_y and Δ_z are the space increments in the y and z coordinate directions, Δ_t is the time increment, and ε_0 and μ_0 are, respectively, the permittivity and the permeability of free space.

For deriving the update equations of the magnetic fields, we just modify the coefficients of electric field components connected with the inner loop based on the following reasons: 1) Conformal mesh-generating technique for the high-order FDTD(2,4) scheme is the same with the traditional low-order locally conformal technique [3]. 2) The electric field components connected with the inner loop place more important part in updating the magnetic field components than those connected with the outer loop.

The general Faraday's law can be written as

$$\frac{1}{\sqrt{\mu_0\varepsilon_0}}\oint_L \hat{\mathbf{E}}\cdot d\mathbf{L} = -\frac{\partial}{\partial t}\int\int_S \mathbf{H}\cdot d\mathbf{S}. \tag{5}$$

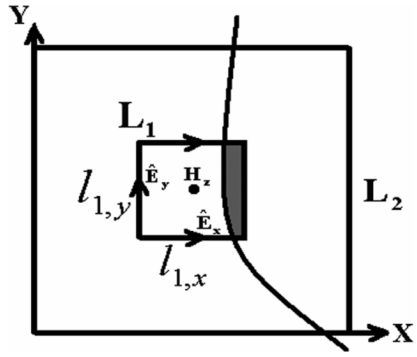

Fig. 1. The general Faraday's loops for the staggered FDTD(2,4) method. The dot denotes H_z. The four electric field components near from H_z link the inner loop L_1, and those far from H_z link the outer loop L_2. $l_{1,x}$ and $l_{1,y}$ are the side lengths along the x and y directions outside the perfectly conducting object. The gray region denotes the region inside the object.

Applying (5) and the locally conformal technique [3] to the inner loop L_1, we can get

$$\begin{aligned} H_z^{n+1/2}&\left(i+\frac{1}{2},j+\frac{1}{2},k\right) \\ &= H_z^{n-1/2}\left(i+\frac{1}{2},j+\frac{1}{2},k\right)+\frac{1}{\sqrt{\mu_0\varepsilon_0}}\times\frac{\Delta_t}{\Delta S_1^*} \\ &\times\left\{+\left[\hat{E}_x^n\left(i+\frac{1}{2},j+1,k\right)l_{1,x}(i,j+1,k)\right.\right. \\ &\qquad\left.-\hat{E}_x^n\left(i+\frac{1}{2},j,k\right)l_{1,x}(i,j,k)\right] \\ &\quad-\left[\hat{E}_y^n\left(i+1,j+\frac{1}{2},k\right)l_{1,y}(i+1,j,k)\right. \\ &\qquad\left.\left.-\hat{E}_y^n\left(i,j+\frac{1}{2},k\right)l_{1,y}(i,j,k)\right]\right\} \end{aligned} \tag{6}$$

where $l_{1,x}$ and $l_{1,y}$ are the side lengths along the x and y directions outside the perfectly conducting object, and ΔS_1^* is the area of the modified inner loop L_1 outside the object (see Fig. 1).

The outer loop L_2 is unmodified, and (5) can be converted to

$$\begin{aligned} H_z^{n+1/2}&\left(i+\frac{1}{2},j+\frac{1}{2},k\right) \\ &= H_z^{n-1/2}\left(i+\frac{1}{2},j+\frac{1}{2},k\right)+\frac{1}{3} \\ &\times\left\{+CFL_y\times\left[\hat{E}_x^n\left(i+\frac{1}{2},j+2,k\right)\right.\right. \\ &\qquad\left.-\hat{E}_x^n\left(i+\frac{1}{2},j-1,k\right)\right] \\ &\quad-CFL_x\times\left[\hat{E}_y^n\left(i+2,j+\frac{1}{2},k\right)\right. \\ &\qquad\left.\left.-\hat{E}_y^n\left(i-1,j+\frac{1}{2},k\right)\right]\right\}. \end{aligned} \tag{7}$$

Considering that the integral form of Maxwell's equations is identical to the differential form of Maxwell's equations, the update equation for H_z field can be obtained by adding (6) multiplied by 9/8 to (7) multiplied by $-1/8$, i.e.,

$$\begin{aligned} H_z^{n+1/2}&\left(i+\frac{1}{2},j+\frac{1}{2},k\right) \\ &= H_z^{n-1/2}\left(i+\frac{1}{2},j+\frac{1}{2},k\right)+\frac{\Delta_t}{\sqrt{\mu_0\varepsilon_0}\Delta S_1^*}\times\frac{9}{8} \\ &\times\left\{\left[\hat{E}_x^n\left(i+\frac{1}{2},j+1,k\right)l_{1,x}(i,j+1,k)\right.\right. \\ &\qquad\left.-\hat{E}_x^n\left(i+\frac{1}{2},j,k\right)l_{1,x}(i,j,k)\right] \\ &\quad-\left[\hat{E}_y^n\left(i+1,j+\frac{1}{2},k\right)l_{1,y}(i+1,j,k)\right. \\ &\qquad\left.\left.-\hat{E}_y^n\left(i,j+\frac{1}{2},k\right)l_{1,y}(i,j,k)\right]\right\}-\frac{1}{24} \\ &\times\left\{CFL_y\times\left[\hat{E}_x^n\left(i+\frac{1}{2},j+2,k\right)\right.\right. \\ &\qquad\left.-\hat{E}_x^n\left(i+\frac{1}{2},j-1,k\right)\right]-CFL_x \\ &\quad\times\left[\hat{E}_y^n\left(i+2,j+\frac{1}{2},k\right)\right. \\ &\qquad\left.\left.-\hat{E}_y^n\left(i-1,j+\frac{1}{2},k\right)\right]\right\}. \end{aligned} \tag{8}$$

To obtain stable and accurate numerical results, we set

$$\Delta S_1^*=\begin{cases}\Delta S_1^*, \Delta S_1^*\geq\gamma\Delta S_1\\ \gamma\Delta S_1, \Delta S_1^*<\gamma\Delta S_1\end{cases} \tag{9}$$

where ΔS_1 is the constant area of the unmodified inner loop L_1, and γ is the threshold. The smaller γ results in better numerical precision but smaller time increment to ensure the stability of the scheme.

Under uniform space increment condition, a rigorous global stability limit for the 3-D scattering problems can be given as

$$\Delta_t\leq\frac{\sqrt{\varepsilon_0\mu_0}\Delta_x}{\sqrt{3}\times\left|\frac{1}{24}+\frac{9}{8}\cdot\frac{\max_\nu(l_{1,\nu})\Delta_x}{\Delta S_1^*}\right|},\quad\forall\, L_1 \tag{10}$$

where $\max_\nu(l_{1,\nu})$ is the maximum length of the four sides connected with the inner loop L_1.

III. Numerical Results

Without loss of generality, we assume that a plane wave of frequency 300 MHz travels along the z direction, the electric field is polarized along the x direction, and the uniform space increment is adopted. The threshold γ is set to be 0.01, the Courant-Friedrichs-Levy (CFL) number is chosen as 0.25, and 10-layered perfectly matched layer(PML) is employed to absorb the outgoing wave. Furthermore, to obtain accurate far-field results, the high-order near-to-far-field (NFF) transformation [10] and the trick reported in [11] are adopted.

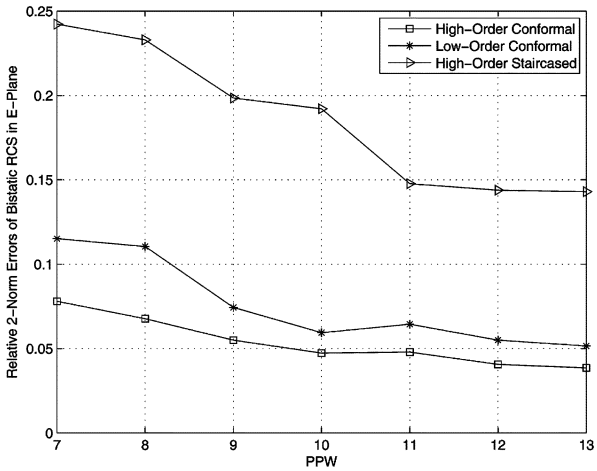

Fig. 2. Relative two-norm errors of bistatic RCS in E-plane for the low-order conformal method, the high-order staircasing approach, and the high-order conformal scheme. (MoM solution is used as reference solution).

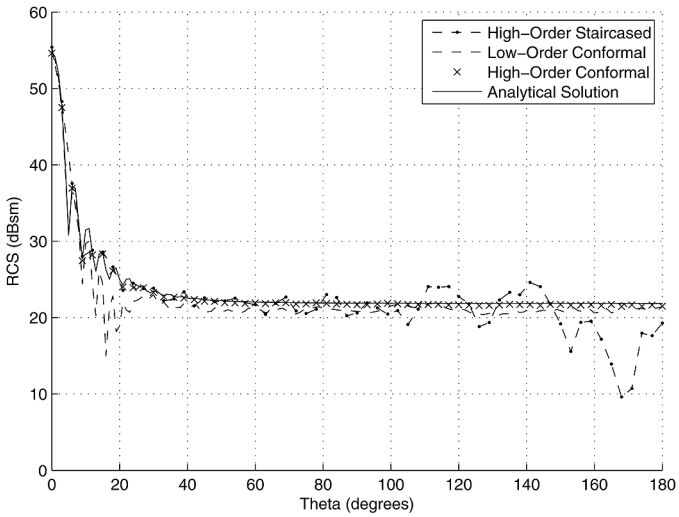

Fig. 3. H-plane bistatic RCS of the conducting sphere calculated by the low-order conformal method, the high-order staircasing approach, and the high-order conformal scheme.

The scattering from electrically-small conducting circular cylinder of height 2 m and radius 1 m is considered. The symmetrical axis of the cylinder is placed along the y direction. Fig. 2 shows the relative two-norm errors of bistatic radar cross section (RCS) as a function of points per wavelength (PPW). It can be seen that the high-order conformal scheme can obtain better numerical precision than the high-order staircasing approach and the low-order conformal method.

The next example considered is the scattering from electrically-large conducting sphere of diameter 14 m. In particular, we use only 7 PPW to model the curved surfaces. From Fig. 3, compared with the low-order conformal method and the high-order staircasing approach, the high-order conformal scheme agrees with the analytical solution very well. The relative two-norm errors of bistatic RCS in H-plane for the low-order conformal method, the high-order staircasing approach, and the high-order conformal scheme are, respectively, 7.3%, 12.3%, and 0.85%.

TABLE I
CONSUMED CPU TIME AND MEMORY UNDER THE SAME RELATIVE TWO-NORM ERRORS CONDITION

Algorithm	PPW	CFL Number	CPU time (s)	Memory (MB)
High-order Conformal	7	0.25	3927	258
High-order Staircased	16	0.45	13288	1318
Low-order Conformal	13	0.30	9175	820

Under the same relative two-norm errors condition, we change the settings of the space increment and the CFL number, and the CPU time and memory consumed by different algorithms are recorded in Table I.

IV. CONCLUSION

Using the locally conformal technique and the fourth-order staggered difference, the high-order conformal FDTD(2,4) scheme is accurate and efficient for modeling the scattering from 3-D curved perfectly conducting objects. In addition, the decreased time increment caused by the conformal model can be offset by using coarse grids.

REFERENCES

[1] K. S. Yee, "Numerical solution of initial boundary value problems involving Maxwell's equations in isotropic media," *IEEE Trans. Antennas Propag.*, vol. AP-14, no. 3, pp. 302–307, Mar. 1966.

[2] T. G. Jurgens, A. Taflove, K. Umashankar, and T. G. Moore, "Finite-difference time-domain modeling of curved surfaces," *IEEE Trans. Antennas Propag.*, vol. 40, no. 3, pp. 357–366, Apr. 1992.

[3] S. Dey and R. Mittra, "A locally conformal finite-difference time-domain (FDTD) algorithm for modeling three-dimensional perfectly conducting objects," *IEEE Microw. Guided Wave Lett.*, vol. 7, no. 9, pp. 273–275, Sep. 1997.

[4] W. H. Yu and R. Mittra, "A conformal FDTD algorithm for modeling perfectly conducting objects with curve-shaped surfaces and edges," *Microw. Optical Technol. Lett.*, vol. 27, pp. 136–138, 2000.

[5] I. A. Zagorodnov, R. Schuhmann, and T. Weiland, "A uniformly stable conformal FDTD-method in cartesian grids," *Int. J. Numer. Modelling-Electron. Networks Devices Fields*, vol. 16, pp. 127–141, 2003.

[6] T. Xiao and Q. H. Liu, "Enlarged cells for the conformal FDTD method to avoid the time step reduction," *IEEE Microw. Wireless Compon. Lett.*, vol. 14, no. 12, pp. 551–553, Dec. 2004.

[7] J. Fang, "Time Domain Finite Difference Computation for Maxwell's Equations," Ph.D., Univ. California, Berkeley, CA, 1989.

[8] A. Yefet and P. G. Petropoulos, "A staggered fourth-order accurate explicit finite difference scheme for the time-domain Maxwell's equations," *J. Computat. Phys.*, vol. 168, pp. 286–315, 2001.

[9] S. V. Georgakopoulos, C. R. Birtcher, C. A. Balanis, and R. A. Renaut, "HIRF penetration and PED coupling analysis for scaled fuselage models using a hybrid subgrid FDTD(2,2)/FDTD(2,4) method," *IEEE Trans. Electromagn. Compat.*, vol. 45, no. 2, pp. 293–305, May 2003.

[10] W. Sha, Z. X. Huang, X. L. Wu, and M. S. Chen, "Application of the symplectic finite-difference time-domain scheme to electromagnetic simulation," *J. Computat. Phys.*, vol. 225, pp. 33–50, 2007.

[11] X. Li, A. Taflove, and V. Backman, "Modified FDTD near-to-far-field transformation for improved backscattering calculation of strongly forward-scattering objects," *IEEE Antennas Wireless Propag. Lett.*, vol. 4, pp. 35–38, Jun. 2005.